Microscopic origin of room-temperature ferromagnetism in the double perovskite Sr_2FeReO_6

Shishir K. Pandey,[1,2,3] Ashis K. Nandy,[1,4] Poonam Kumari,[1] and Priya Mahadevan[1,*]

[1]*Department of Condensed Matter Physics and Material Science, S. N. Bose National Center for Basic Sciences, Kolkata-700106*

[2]*International Center for Quantum Materials, School of Physics, Peking University, Beijing 100871, China*

[3]*Artificial Intelligence for Science Institute, Beijing, China*

[4]*School of Physical Sciences, National Institute of Science Education and Research, An OCC of Homi Bhabha National Institute, Jatni-752050, India*

(Received 2 February 2022; accepted 27 May 2022; published 21 June 2022)

The puzzling observation of room temperature ferromagnetism in double perovskites ($A_2\,BB'O_6$), despite having the magnetic lattice of B ions diluted by nonmagnetic B' ions, have been examined for Sr_2FeReO_6. *Ab initio* spin spiral electronic structure calculations along various high symmetry directions in reciprocal space are used to determine the exchange interactions entering an extended Heisenberg model, which is then solved classically using Monte Carlo simulations to determine the ferromagnetic transition temperature T_c. We find that one must consider on-site Coulomb interactions at the nonmagnetic Re sites (U) in order to obtain a T_c close to the experimental value. Analysis of the *ab initio* electronic structure as well as an appropriate model Hamiltonian trace the origin of enhancement in T_c with U to the enhanced exchange splitting that is introduced at these sites. This in turn destabilizes the antiferromagnetic exchange channels, thereby enhancing the T_c. The role of occupancy at the nonmagnetic sites is examined by contrasting with the case of Sr_2FeMoO_6.

DOI: 10.1103/PhysRevB.105.214422

I. INTRODUCTION

Double perovskite (DP) oxides have the general formula $A_2\,BB'O_6$ with A being the rare earth or alkaline-earth ion, B and B' are the transition metal atoms separated by oxygen atoms in the lattice. In general, a DP oxide consists of two sublattices of perovskite ABO_3 and $AB'O_3$ units in a way that the B and B' sites are arranged alternately in a three- dimensional array. B (B') transition metal atoms reside in an octahedra formed by six oxygen atoms. The finding of ferromagnetic behavior in the Re based DP oxides A_2FeReO_6 (where A = Ba, Sr, Ca) above room temperature (with ferromagnetic transition temperatures 316, 401, and 538 K, respectively) [1] stimulated research in this new ferromagnetic class of DP oxides. Another similar example of a high T_c ferromagnetic DP oxide is Sr_2FeMoO_6 (SFMO) with a transition temperature of 410 K [2,3]. In Sr_2FeReO_6 (SFRO), the separation between the closest magnetic Fe atoms is $\sqrt{2}$ times larger than that found in a Fe-based perovskite oxide. This large separation of Fe atoms arises because of the dilution of the magnetic lattice with nonmagnetic Re atoms. The naive expectation was that it should result in weaker magnetic interactions and hence a lower magnetic ordering temperature. Surprisingly, the Curie temperature for this system is 401 K. In contrast, considering the case of the hole doped manganites [4], where one has smaller separations between the magnetic atoms, one finds a lower magnetic ordering temperature. As the ferromagnetism has been conventionally understood within a double exchange model, the presence of nonmagnetic atoms like Re/Mo present in a double perovskite crystal requires a different mechanism to explain the high ferromagnetic ordering temperature in these compounds.

A qualitative model to understand the high magnetic ordering temperature was proposed by Sarma *et al.* [5] after analyzing the *ab initio* electronic structure of SFMO. They concluded that the hopping interactions between first neighbor Fe and Mo atoms in the lattice led to an exchange splitting being induced on the Mo sites which is opposite in direction to that at the Fe site. This led to an antiferromagnetic coupling between the Fe and Mo sites and an effective ferromagnetic coupling between the Fe sites. This results in the high magnetic ordering temperatures of these materials.

Electronic structure calculations reveal that the majority Fe up spin t_{2g} and e_g states are ∼3.75 and 2.25 eV below the Fermi energy, respectively, while the minority spin states have highly hybridized Fe-Re/Mo character. This idea led to the use a Kondo-like model to describe the magnetism in these materials. The majority spin Fe states are approximated by a spin within this model which interacts with the itinerant conduction electrons through an antiferromagnetic coupling. The itinerant conduction electron can delocalize by hopping from the t_{2g} levels on the nonmagnetic transition metal atom to those on Fe. While this model was able to successfully explain the high magnetic ordering temperature in Sr_2FeMoO_6 which had just one electron on the nonmagnetic atom, it failed to explain the high magnetic ordering temperature when one had more than one electron on the nonmagnetic atom as in Sr_2FeReO_6 [6–9].

Brey and coworkers [10] carried out a mean-field study considering a t_{2g} only model. The suppression of T_c was recovered qualitatively by introducing electron-electron

*priya.mahadevan@gmail.com

 ©2022 American Physical Society

interactions at the nonmagnetic site within the model. This helped in obtaining the experimental trend of increase in T_c with increase of the number of electrons at the nonmagnetic site. We reexamine the changes in the electronic structure at the nonmagnetic site, examining how it evolves with U and how this affects the stability of the ferromagnetic state with respect to the competing antiferromagnetic state, in addition to the modifications in the exchange interaction strengths.

In this context, the issue of high temperature magnetism in Sr_2FeReO_6 has been studied within *ab initio* electronic structure as well as a model Hamiltonian approach. The *ab initio* band structure calculations were performed and electron correlation effects on Fe as well as on Re sites were introduced within the generalized gradient approximation (GGA)+U technique. Considering a U of 2.5 eV on the Fe site, the ground state is found to be ferromagnetic. The magnetic exchange interaction strengths (J)'s between the magnetic (Fe) atoms were calculated using an inverse Fourier transform method. Using a classical Monte Carlo (MC) simulation technique employing an extended Heisenberg model, the T_c of the system was estimated. In the first case, when there was no U on the Re site, we found that the nearest-neighbor exchange interaction J_1 is ferromagnetic, while the second-neighbor exchange interaction J_2 is antiferromagnetic contrary to what is believed in literature [11]. J_3 and J_4 are negligibly small when compared to J_1, J_2. With these exchange interaction strengths, the estimated T_c within the MC simulation study was much lower ($\sim$285 K) than the experimental value of 401 K. Taking a clue from the work by Brey *et al.* [10], we then considered a U of 1 eV on the Re d states and again calculated the exchange interaction strengths. We found that the J_1 got enhanced by a factor of $\sim$2. Most surprisingly, J_2 changes its sign from being antiferromagnetic in the no U case to ferromagnetic in the present case when a U of 1 eV is considered at the Re site. Using a U(Fe) = 2.5 eV and U(Re) = 1.0 eV, we find the magnetic ordering temperature to be 395 K, which is reasonably close to the experimentally observed value. Within *ab initio* electronic structure calculations, the ferromagnetic ground state is found to be half-metallic. The Re moments found in this case are induced in nature and are antiparallel to Fe moments. With an application of U on the Re site, we found no substantial effect in the density of states for the ferromagnetic configuration that could explain the gain in stability in this case. However, examining the density of states in a competing antiferromagnetic configuration we found that the U(Re) played the role of inducing an exchange splitting of the Re d states. Thus by destabilizing the antiferromagnetic state, we found that one could increase the ferromagnetic stability. In order to test this hypothesis we set up a multiband Hubbard Hamiltonian to describe the system. Introducing an exchange splitting (J_h) on Re was found to enhance the stability of the ferromagnetic state.

II. METHODOLOGY

The electronic and magnetic properties of SFRO have been calculated using a plane wave pseudopotential implementation of density functional theory using projected augmented plane wave potentials [12,13] implemented in the Vienna *ab initio* simulation package (VASP). The GGA [14,15] has been used for the exchange correlation functional. The effects of electron-electron correlation on the transitional metal d electrons were considered within the GGA + U scheme using the Dudarev *et al.* formalism [16] for the plus U implementation. In our calculations we have used a U of 2.5 eV on the Fe d states while a U of 0, 1 and 2 eV was considered on the Re d states. A k mesh of $8\times8\times8$ was used for the integrations in momentum space, while a cutoff energy of 500 eV was used for the plane wave included in the basis for the calculations. The interatomic exchange interactions strengths J's were determined using the frozen magnon approach [17–20]. In this approach the total energy corresponding to each spin spiral state associated with a spin spiral vector $\vec{q}$ was calculated within a noncollinear spin implementation in VASP [21]. Each spin at the Fe site is treated classically and treated as a vector where $\vec{s}_i$ is a unit vector along the direction of the spin at the site labeled by i. Hence,

$$\vec{s}_i = (\sin\theta\cos(\vec{q}\cdot\vec{R}_i), \sin\theta\sin(\vec{q}\cdot\vec{R}_i), \cos\theta), \tag{1}$$

where $\vec{R}_i$ is the position of the atom and θ is the polar angle made by the spin with the z axis. Assuming the spins at the Fe sites to be localized, we mapped the magnetic energies calculated for various $\vec{q}$ onto an extended Heisenberg model as,

$$H = -\frac{1}{2}\sum_{ij} J_{ij}\vec{s}_i\cdot\vec{s}_j. \tag{2}$$

The use of Heisenberg model in this mapping is justified as the largest deviation of Fe magnetic moments for different values of $\vec{q}$ from the $\vec{q}=0$ value remains less than 1.1%. In the above equation, s_i, s_j are unit vectors in the direction of the spins at sites i and j while J_{ij} are the exchange interaction strengths between the Fe spins at site i and j. The magnitude of spins are absorbed into the J. It is clear that in this model, positive and negative J value imply ferromagnetic and antiferromagnetic exchange interactions respectively. Hence, corresponding to each $\vec{q}$ value, one has the total energy $E(\vec{q})$ in terms of the $J(\vec{q})$ which is related to the exchange interactions via Fourier transformation as,

$$J(\vec{q}) = \sum_{i\neq0} J_{0i}e^{i\vec{q}\cdot\vec{R}_{0i}}. \tag{3}$$

For simplicity, in our calculations, we restricted the spins to lie in the xy plane. After performing an inverse Fourier transform, we obtain the real space exchange parameters as

$$J_{0i} = \frac{1}{N}\sum_{\vec{q}} J(\vec{q})e^{-i\vec{q}\cdot\vec{R}_{0i}}. \tag{4}$$

Thus the calculated spin wave spectra along various various high symmetry directions with varying $\vec{q}$ has been determined and the spectrum was fitted using a least squares error minimization procedure to estimate the exchange parameters with the best fit. The Boltzmann weight factor $e^{-\beta\Delta E}$ was considered while estimating the exchange parameters to take care of the fact that statistical weight corresponding to large angles between the spins are low in the frozen magnon states. Here $\beta = 1/k_BT$ where T is the ferromagnetic transition temperature of 401 K for SFRO and $\Delta E = E(\vec{q}) - E(0)$ [22]. This

analysis was done for both the case when there was no U on the Re sites and also with a $U(\mathrm{Re}) = 1$ eV while the U on Fe sites was kept fixed at 2.5 eV.

With the help of these exchange interactions, we have calculated the ferromagnetic transition temperature (T_c) using a classical MC [23] method. In this technique, we first set up the magnetic lattice. In SFRO the Fe atoms form a face-centered lattice. A system size consisting of $16\times16\times16$ spins is considered. The extracted J's from the procedure discussed above are used as inputs for an extended Heisenberg model. During a single MC run, random orientations ($\vec{s}_i$) for a spin at i th site were considered and the energy of the system was calculated. Then a new random orientation of spin ($\vec{s}_i'$) was created and the system energy was again calculated. If the energy associated with this new random orientation ($\vec{s}_i'$) was lower than that of ($\vec{s}_i$), then ($\vec{s}_i'$) was accepted. Otherwise, the Metropolis algorithm [24] was employed to decide whether to accept or reject ($\vec{e}_i'$). This procedure was performed over all the lattice sites i is one Monte Carlo step. The magnetization M(T) per spin was calculated only after bringing the system into thermal equilibrium. A total of 5×10^5 Monte Carlo steps were used in these calculations and results were found to be well converged with respect to the system size as well as the MC steps.

The multiband Hubbard Hamiltonian considered for the microscopic understanding of the system is given as

$$
\begin{aligned}
H = &\sum_{i,l,\sigma} \epsilon_d^f d_{il\sigma}^\dagger d_{il\sigma} + \sum_{i,l,\sigma} \epsilon_d^m d_{il\sigma}^\dagger d_{il\sigma} + \sum_{i,l,\sigma} \epsilon_p p_{il\sigma}^\dagger p_{il\sigma} \\
&+ \sum_{i,l,\sigma} \epsilon_s s_{il\sigma}^\dagger s_{il\sigma} - \sum_{i,j,l_1,l_2,\sigma} \left(t_{i,j,pd_f}^{l_1 l_2} d_{il_1\sigma}^\dagger p_{jl_2\sigma} + \mathbf{H.c.}\right) \\
&- \sum_{i,j,l_1,l_2,\sigma} \left(t_{i,j,pd_m}^{l_1 l_2} d_{il_1\sigma}^\dagger p_{jl_2\sigma} + \mathbf{H.c.}\right) \\
&- \sum_{i,j,l_1,l_2,\sigma} \left(t_{i,j,pp}^{l_1 l_2} p_{il_1\sigma}^\dagger p_{jl_2\sigma} + \mathbf{H.c.}\right) \\
&- \sum_{i,j,l_1,l_2,\sigma} \left(t_{i,j,sd_f}^{l_1 l_2} d_{il_1\sigma}^\dagger s_{jl_2\sigma} + \mathbf{H.c.}\right) \\
&- \sum_{i,j,l_1,l_2,\sigma} \left(t_{i,j,sd_m}^{l_1 l_2} d_{il_1\sigma}^\dagger s_{jl_2\sigma} + \mathbf{H.c.}\right) \\
&+ \sum_{\alpha\beta\gamma\delta,\sigma_1\sigma_2\sigma_3\sigma_4} U_{dd,f}^{\alpha\beta\gamma\delta} d_{\alpha\sigma_1}^\dagger d_{\beta\sigma_2}^\dagger d_{\gamma\sigma_3} d_{\delta\sigma_4} \\
&+ \sum_{\alpha\beta\gamma\delta,\sigma_1\sigma_2\sigma_3\sigma_4} U_{dd,m}^{\alpha\beta\gamma\delta} d_{\alpha\sigma_1}^\dagger d_{\beta\sigma_2}^\dagger d_{\gamma\sigma_3} d_{\delta\sigma_4},
\end{aligned}
$$

where $d_{il\sigma}^\dagger (d_{il\sigma})$ creates (annihilates) an electron with spin σ in the lth d orbital on transition metal site in the ith unit cell while $p_{il\sigma}^\dagger (p_{il\sigma})/s_{il\sigma}^\dagger (s_{il\sigma})$ creates (annihilates) an electron with spin σ in the lth p/s orbital on oxygen atom in the ith unit cell. Here the index f and m represent the Fe and Re sites, respectively. The hopping interaction strengths (t) were kept fixed at the values obtained from fitting the nonmagnetic *ab initio* band structure of Sr_2FeReO_6 within a tight-binding model having Fe d, Re d and O s and p states in the basis. These hopping interactions were parametrized in terms of Slater-Koster parameters [25] $dp\sigma$, $dp\pi$, $pp\sigma$, $pp\pi$, and $ds\sigma$.

TABLE I. Experimental and optimized/theoretical structural details for Sr_2FeReO_6. In the second and third column, experimental details are given for cubic [26] and tetragonal [27] structures, respectively. Fe-O and Re-O bond lengths are quite similar for the experimental tetragonal phase and our optimized crystal structure of Sr_2FeReO_6 phase.

Structural details	Experimental	Experimental	Theoretical
Space group	Fm-3 m	I 4/m	Fm-3 m
$a = b$ (Å)	7.888 (=c)	5.561	7.890 (=c)
c (Å)	–	7.901	–
$\alpha = \beta = \gamma$ (°)	90	90	90
Bond lengths (Å)			
Re-O	1.70	1.959/1.962	1.94
Fe-O	2.24	1.985/1.991	2.01
Fe-O-Mo Bond angles (in degrees)			
In-plane	180	170	180
Out-of-plane	180	180	180
Cell volume (Å^3)	490.8	488.8	491.17

The on-site energies were however varied, though the same values were taken for both spin channels. The Coulomb matrix elements were parameterized in terms of the Slater-Condon integrals [28] F^0, F^2, and F^4 exploiting its rotationally invariant nature and their values were determined from atomic Hartree-Fock calculations. As the value of F^0 is decreased significantly from its atomic value due to screening, it was varied and used to determine the multiplet averaged Coulomb interaction U. As the Hund's exchange interaction strength is related to the Slater-Condon integrals by the relation $J_h = \frac{F^2+F^4}{14}$, a reduction factor was used to get the desired exchange splitting observed in the *ab initio* spin polarized calculations. For Fe d orbitals, a value of J_h of 0.8 eV was considered while at the Re site it is varied from 0.24 to 0.4 eV.

The four fermion Coulomb interaction terms in the above Hamiltonian were reduced to quadratic terms assuming a mean-field approximation [29–31]. The expectation values of the order parameters entering the mean field decoupled Hamiltonian were determined self-consistently till an energy convergence of 10^{-5} eV was achieved. Total energy and density of states were calculated using the tetrahedron method of integration for a $10\times10\times10$ k mesh.

III. RESULTS AND DISCUSSION

An ordered double perovskite structure consists of two different transition metal atoms B and B' arranged alternately, each with a local environment involving BO_6 and $B'O_6$ octahedra. The crystal structure of Sr_2FeReO_6 is simple cubic with space group Fm-$3m$ [26]. We have optimized both the unit cell parameters as well as the internal positions within *ab initio* electronic structure calculations with $U(\mathrm{Fe}) = 2.5$ eV. The theoretically optimized structural information are given in Table I.

The experimental unit cell parameters are also given for comparison. As one can see, in SFRO all the Fe-O-Re bond lengths are 180° while all the Fe-O or Re-O bond lengths are identical within the respective octahedra as is evident

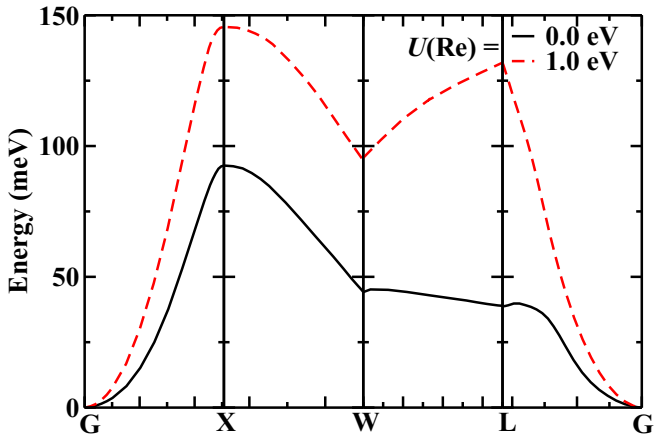


FIG. 1. Magnon dispersion plot for Sr_2FeReO_6 for U(Fe) = 2.5 eV and U(Re) = 0 and 1 eV. The G-point energy is the ferromagnetic ground state energy which gets higher stability with application of $U = 1$ eV on the Re site.

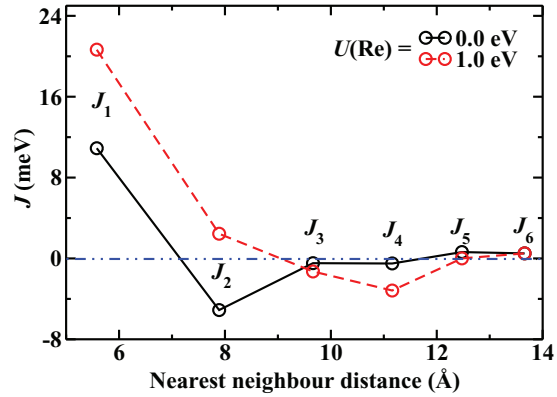


FIG. 2. Fe-Fe interatomic exchange interaction parameters (J) of Sr_2FeReO_6 as a function Fe-Fe nearest-neighbor distance (in Å).

from Table I. Further there was no substantial change in the experimentally observed lattice constants found after structural optimization. However, there is substantial change in the Fe-O and Re-O bond lengths after the optimization. We use this optimized structure in the rest of our calculations. Obtained Fe-O and Re-O bond lengths in for our optimized structure is quite similar to the ones found in the tetragonal phase of Sr_2FeReO_6. This similarity among the bond lengths of the tetragonal crystal structure along with the fact that the tetragonal distortion is quite small in magnitude (∼0.011 Å) justify use of optimized crystal structure in our calculations. To understand the high magnetic ordering temperature of this system, the magnon dispersions were calculated along various symmetry directions in the Brillouin zone of SFRO (Fig. 1). Each point in Fig. 1 corresponds to a different magnetic configuration identified by $\vec{q}$ and has been calculated for a U of 2.5 eV on the Fe d states. Clearly, $\vec{q} = 0$, (G point) which represents the ferromagnetic state has the lowest energy.

This is in agreement with the experimental findings. The value of magnetic moment at Fe and Re sites are 3.9 μ_B and -0.95 μ_B, respectively. This reasonably large magnetic moment of -0.95 μ_B on the Re site which is usually regarded as nonmagnetic seems surprising. The intra-atomic Hunds exchange interaction strength responsible for spin polarization, is much smaller for Re 5d orbitals than for the 3d orbitals. This coupled with the large bandwidths associated with the Re 5d orbitals would have us expect a small magnetic moment at the Re site. The large moment is an induced moment which arises from hopping of electrons between the Fe d and the Re d states as discussed in Ref. [5]. This leads to a ferromagnetic coupling between the Fe spins, and is responsible for stabilizing the ferromagnetic state. This is evident from the density of states calculated for a perfectly antiferromagnetic configuration. In that case one had no exchange splitting of the Re d states, which one would otherwise find if there was a component emerging from an intrinsic exchange splitting.

The real space exchange interaction strengths (Js) are then estimated from an inverse Fourier transformation. A plot of the different Js as a function of distance is given in Fig. 2.

We found that in this case when there is no U on the Re d states, J_1, which is the most dominant one, was found to be 10.9 meV and is ferromagnetic while J_2 is -5.1 meV and is antiferromagnetic in nature. All other Js are negligibly small. A schematic showing the first four exchange interactions and the pathways they represent is shown in Fig. 3. One should mention here that the separation between the Fe atoms connected via J_1, J_2, J_3, and J_4 are ∼5.58, 7.89, 9.66, and 11.16 Å respectively. Using these values for the exchange interaction strengths in a Monte Carlo calculation, one finds a magnetic transition temperature of 285 K. As shown by Brey *et al.*, application of U on the nonmagnetic Mo site will penalize double occupancy. It consequently leads to the ferromagnetic state being favored. Taking a clue from this hypothesis, we applied a U of 1 eV on the Re d states while a U on Fe d states was kept fixed at the value of 2.5 eV and recalculated the magnon spectra shown in Fig. 1 (red dashed lines). A plot of estimated values of Js in this case is shown in Fig. 2.

A clear enhancement in the stability of the ferromagnetic configuration can be found in this case when compared to the

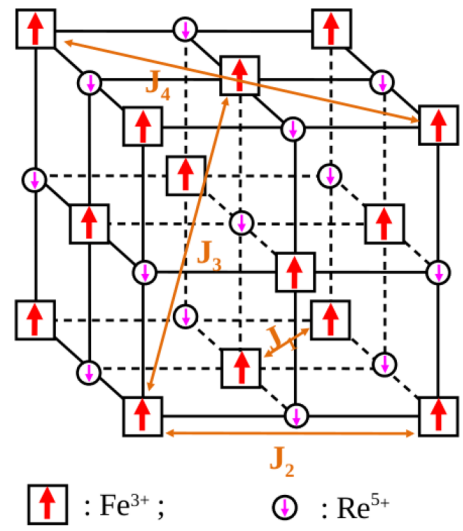


FIG. 3. A schematic to show the first four Fe-Fe interatomic exchange interaction strengths (Js) in the simple cubic lattice of Sr_2FeReO_6.

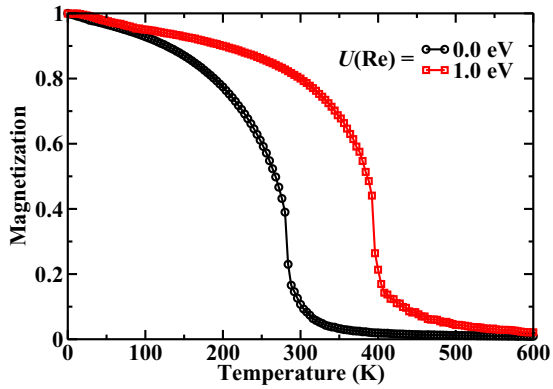


FIG. 4. Variation of normalized magnetization as a function of temperature calculated for $U(\mathrm{Fe}) = 2.5$ eV and $U(\mathrm{Re}) = 0$ and 1 eV using MC simulations for Sr_2FeReO_6.

previous case of no U on Re. The effect of U on the Re site is also manifested in the exchange parameters. An analysis of the estimated Js in this case yields mainly two important points. First is the enhancement in the magnitude of the most dominant nearest-neighbor ferromagnetic exchange interaction strength J_1. Its value ∼21 meV is nearly doubled with a $U(\mathrm{Re}) = 1$ eV from its value in the absence of U on Re. Most interestingly, J_2 which was antiferromagnetic in the previous case is now found to be ferromagnetic in the present case. The estimated T_c with this new set of exchange interaction strengths is 395 K which is in reasonable agreement with the experimental value of 401 K. The magnetic moment on the Re site is enhanced to -1.04 μ_B in this case while it is the same for the Fe atoms when there was no U on the Re d states. A plot of the normalized magnetic moment variation as a function of temperature in both the cases when there is no U on Re and when a U of 1 eV is considered on the Re d states is shown in Fig. 4. There is indeed a clear enhancement of the T_c.

To explain the role of a U on the Re d states, we went to examine the Fe and Re atom projected density of states in both the cases with and without a U on Re d states for the ferromagnetic ground states, a plot of which is shown in left panel of Fig. 5. We also include the case where a U of

TABLE II. Change in stability of the ferromagnetic state calculated with respect to closest competing antiferromagnetic state from *ab initio* calculations as function of U on the Re/Mo d states for Sr_2FeReO_6 and Sr_2FeMoO_6 double perovskites.

	ΔE [AFM-FM] (eV)	
U (eV)	Sr_2FeReO_6	Sr_2FeMoO_6
0.0	0.085	0.129
1.0	0.138	0.143
2.0	0.175	0.158

2 eV was considered on the Re d states. The large exchange splitting at the Fe site and an induced small exchange splitting at Re site is evident from the plot.

We include the discussion about the Fe d projected partial density of states for continuity, though they have not been shown here. In the up spin channel, Fe states are fully occupied verifying the $3d^5$ ionic configuration of Fe while as one can see the Re states are unoccupied and are ∼0.6 eV above the Fermi level. With the application of U on Re, the unoccupied Re up spin states are pushed up away from the Fermi level. A U of 1 eV on Re pushes the Re d states by ∼0.25 eV from its position for the case when there was no U. In the down spin channel, there is hardly any significant change in Fe and Re d density of states with the variation of U on the Re site. They are found to be pinned to their positions in the absence of U. Thus, the small shifts in the Re up spin density of states above the Fermi energy as function of U on the Re d states alone is therefore insufficient to describe the substantial gain in the stability of the ferromagnetic ground state found by examining the magnon dispersion shown in Fig. 1. For example, the gain is ∼50 meV at the X and W points while it is even more than ∼85 meV at the L point over the $U = 0$ values. We went on to examine the density of states of the closest competing antiferromagnetic state. The spins on the Re site are antiferromagnetically coupled to the spins on the Fe sites. We consider antiferromagnetic configurations in which we have flipped the spin of two out of the six Fe nearest neighbors of a Re atom and made them ferromagnetic. As this is a collinear antiferromagnetic configuration with the

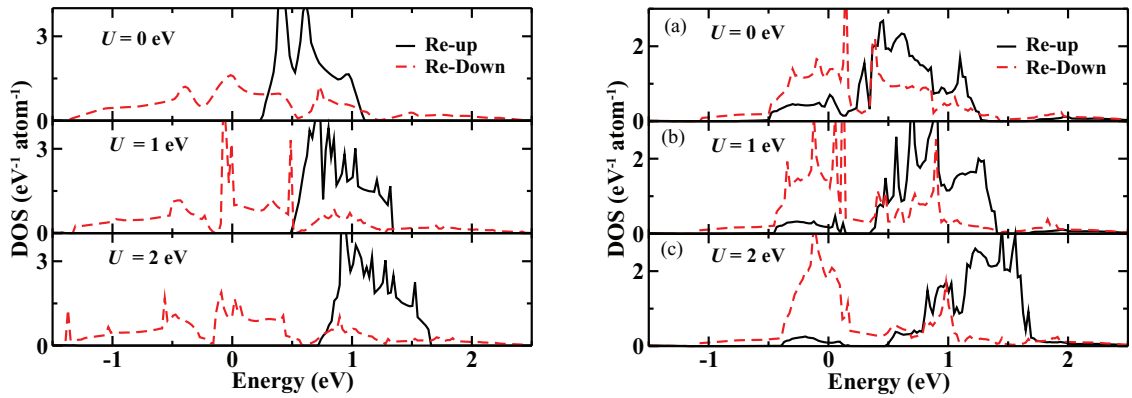


FIG. 5. Atom projected Re d density of states plots from *ab initio* calculations for Sr_2FeReO_6. The plot on the left is for a ferromagnetic configuration of Fe spins while the plot in the right is from the closest competing antiferromagnetic state of Fe spins. The zero of energy is the Fermi energy.

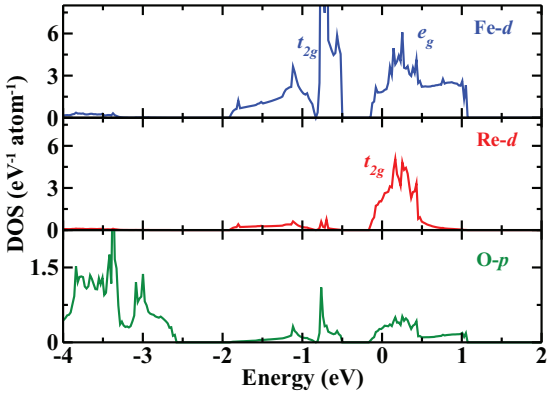


FIG. 6. Fe d, Re d and oxygen p projected partial density of states for nonmagnetic Sr_2FeReO_6 from *ab initio* calculations. The zero of energy is the Fermi energy.

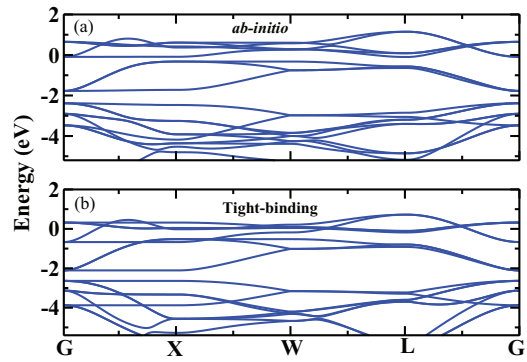


FIG. 7. Nonmagnetic band dispersions from (a) *ab initio*, (b) tight binding calculations with Fe d, Re d and O s and p basis states along various symmetry directions in Brillouin zone of Sr_2FeReO_6. The zero of energy is the Fermi energy.

smallest number of spins around Re flipped, one would expect this to be the closest lying antiferromagnetic excited states.

The atom projected density of states for Fe and Re atoms are then calculated by varying the U on the Re site. The calculated density of states for the Fe d states have almost similar features as found for the ferromagnetic configuration in Fig. 5. Similar to the ferromagnetic case, these states are unaffected by the application of U on Re atom and hence are not shown here. It is the Re d density of states shown in the right panel of Fig. 5, which have the most dramatic effects in this antiferromagnetic configuration with application of U on it. When there is no U on the Re states, both spin channels are found to be contributing at the Fermi level as shown in the right panel (a) of Fig. 5. The induced exchange splitting at the Re site, which was present in the ferromagnetic case has reduced substantially. This provides pathways for both, the ferromagnetically coupled as well as the antiferromagnetically coupled spins. This explains the case of reduced magnetic transition temperature. The Re up spin channel gets substantially depleted at the Fermi level with the application of U on Re d states as shown in the right panel (b) of Fig. 5. The majority weight of the Re up spin states is now much above the Fermi level bringing an effective exchange splitting at the Re site. Because of this the energy gain from delocalization of antiferromagnetically coupled Fe spins is significantly reduced. The exchange splitting at the Re site, further enhances the energy gain for ferromagnetically coupled spins. This is manifested in terms of enhanced J_1 and a ferromagnetic J_2 in this case and consequently a higher T_c. This picture gets even more clear by looking at Re density of states with a U of 2 eV at its d states where the effects are more pronounced. A comparison of the stability of the ferromagnetic states with respect to this antiferromagnetic state as a function of U(Re) is tabulated in Table II.

In order to explicitly understand the role of the exchange splitting at the nonmagnetic Re site, we further went on to develop a simple model which can define this system correctly. For this purpose, we start with calculating the *ab initio* atom projected density of states within a nonmagnetic calculation for Sr_2FeReO_6 and is shown in Fig. 6. The Fe d states are found in the energy window from -2 to 1 eV. The octahedral field of the six oxygens which are the nearest neighbors of Fe lift the degeneracy of the d orbitals and one has the t_{2g} orbitals contributing in the energy window from -2 to -0.5 eV. The e_g states contribute in the energy window from $\sim$0 to 1 eV. We find a similar degeneracy lifting of the d states on Re, with the t_{2g} states contributing in the energy window from $\sim$0 to 0.5 eV. Examining the O p states, one finds that their primary contribution is below ~-3 eV and extends to -8 eV below the Fermi level. There is a small admixture of the O p states in the energy window contributed primarily by the Fe and Re d states. This arises from p-d hybridization and one finds that the contributions are larger for the Fe e_g states as well as the Re t_{2g} states which have the larger hopping matrix elements associated with them. Surprisingly we find the energy window over which the Fe t_{2g} states contribute comparable with that in which Fe e_g states contribute. This seems surprising and could emerge from the smaller energy denominator for the delocalization of an electron in the Fe t_{2g} states via the Re t_{2g} states than the Fe e_g states via the levels with the same symmetry on Re.

The *ab initio* band dispersions along various symmetry directions for nonmagnetic Sr_2FeReO_6 are shown in Fig. 7 in the energy window -4 to 2 eV. As Fe d, Re d and O p

TABLE III. On-site energies and various hopping interaction strengths (in eV) parameterized in terms of Slater-Koster parameters obtained by fitting *ab initio* band structure of nonmagnetic Sr_2FeReO_6 employing a tight-binding model with Fe, Re d and O s and p states in the basis.

On-site energies				Fe-O			Re-O			O-O	
Fe d		Re d	O p	$dp\sigma$	$dp\pi$	$ds\sigma$	$dp\sigma$	$dp\pi$	$ds\sigma$	$pp\sigma$	$pp\pi$
t_{2g}	e_g	t_{2g}									
2.46	3.34	3.90	0.68	1.90	−1.495	−1.44	3.05	−1.28	−0.76	0.75	−0.164

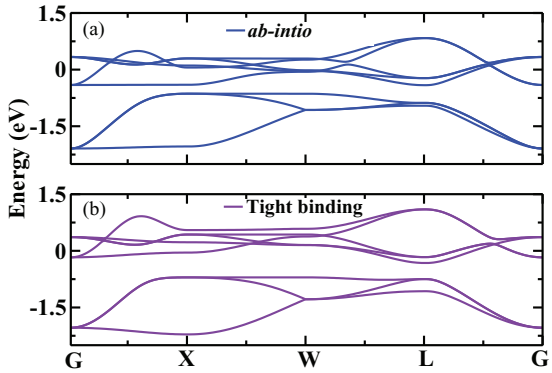


FIG. 8. Nonmagnetic band structure from (a) *ab initio*, (b) tight-binding calculations with only Fe and Re d basis states, plotted along various symmetry directions in Brillouin zone of Sr_2FeReO_6. The zero of energy is the Fermi energy.

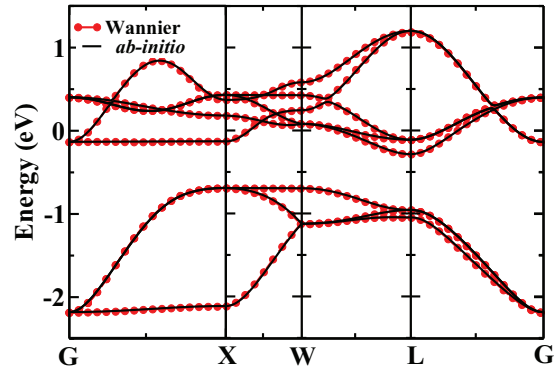


FIG. 9. Nonmagnetic *ab initio* band structure fitted with a Wannier functions based tight- binding model considering Fe and Re d orbitals in the basis. The zero of energy is the Fermi energy.

states were found to contribute in this energy window, we included these states in the basis of the tight-binding model considered. We also included the s states on the oxygen as discussed in the methodology section. The parameters entering the tight-binding Hamiltonian should reproduce the band structure from the *ab initio* calculations. A least- squares error minimization procedure was used [33]. The best fit parameters are given in Table III.

The $dp\pi$ interactions between the Fe d and O p states are significantly enhanced compared to a ratio of 0.5 for $dp\sigma/dp\pi$ interactions that one usually expects explaining partially the similar bandwidths that we find for Fe t_{2g} and Fe e_g states. $ds\sigma$ interactions control the crystal field splitting between the t_{2g} and e_g orbitals and are found to be considerable for the Fe d states also, compared to the Re d states as the Re e_g states were not included in the fitting. Examining the onsite energies, one finds that one has the Fe t_{2g} states, Fe e_g states and then the Re t_{2g} states as expected.

The charge transfer energy between the O p states and Fe t_{2g} states is small but positive. In order to examine the role of explicitly including the O p states in the basis, especially when the charge transfer energy is so small, a mapping was carried out onto a d only model. The parameters found to give the best fit of the *ab initio* band structure shown in Fig. 8(a) are given in Table IV. The tight-binding band structure calculated for the best fit parameters are given in Fig. 8(b).

As is evident, we include explicitly the Fe d and Re d states while constructing the tight- binding Hamiltonian with d-d interactions. Interestingly we find that the Re t_{2g} levels lie in between the Fe t_{2g} and Fe e_g levels. This is because in the effective d only model, we are approximating the positions of the d levels to their positions after their interaction with oxygen. The matrix elements for Fe e_g and O p interactions are larger, resulting in larger shifts compared to the interaction between Re t_{2g} and O p states. This leads to negative energy difference between the Fe e_g and the Re t_{2g} states. In order to verify if the placing of the Re t_{2g} levels below the Fe e_g levels is not an artefact of the fitting procedure, a similar analysis was carried out for a d only mapping using maximally localized Wannier functions [32] for the radial parts of the basis functions. A comparison of the *ab initio* band structure and the fitted band structure are given in Fig. 9.

Here we find that the fit is reasonable, which gives us confidence in examining the on-site energies. We find that the difference between the Re t_{2g} and the Fe e_g levels is negative, ~ -0.7 eV in agreement with what we had earlier. In order to determine the appropriate model, a multiband Hubbard model is considered with the same value of U and the electronic structure for a given set of parameters is calculated using a mean-field decoupling scheme for the four Fermion terms. The hopping interaction strengths are kept fixed at the values obtained by fitting the nonmagnetic band structure.

We consider the charge fluctuations at the Fe and Re sites as

$$\Delta_{Fe-O} = E_f(d^6\bar{L}) - E_i(d^5L^0) = \epsilon_d - \epsilon_p + 5U_{Fe}, \quad (5)$$

$$\Delta_{Re-O} = E_f(d^3\bar{L}) - E_i(d^2L^0) = \epsilon_d - \epsilon_p + 2U_{Re}. \quad (6)$$

Here ϵ_d and ϵ_p are the on-site energies of Fe/Re d and O p orbitals, respectively. Hence Δ was kept fixed with U(Fe)/U(Re) by changing the on-site energies in accordance to the above equations. The J_h are varied till a good

TABLE IV. On-site energies and various hopping interaction strengths (in eV) parameterized in terms of Slater-Koster parameters obtained by fitting *ab initio* band structure of nonmagnetic Sr_2FeReO_6 employing a tight-binding model with only Fe and Re d states in the basis.

On-site energies			Fe-Fe			Fe-Re			Re-Re		
Fe d		Re d	$dd\sigma$	$dd\pi$	$dd\delta$	$dd\sigma$	$dd\pi$	$dd\delta$	$dd\sigma$	$dd\pi$	$dd\delta$
t_{2g}	e_g	t_{2g}									
4.45	6.39	5.10	−0.05	0.05	−0.004	−0.866	0.298	0.0	−0.199	0.008	−0.02

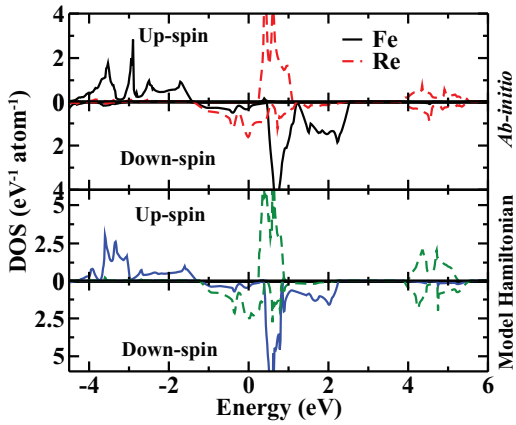


FIG. 10. Atom projected density of states plots from *ab initio* calculations (upper two) and model Hamiltonian calculation (lower two) with Fe and Re d states in the basis of Sr_2FeReO_6. The zero of energy is the Fermi energy.

description of the *ab initio* density of states is obtained. A comparison is shown in Fig. 10.

A J_h of 0.8 eV was considered on Fe and this gave a good description of the *ab initio* density of states. Additionally the charge transfer energy between both Fe and Re with oxygen were found to be 0.85 and 3.5 eV, both positive. Additionally a U of 0.26 eV and a small J of 0.24 eV was used on the Re states to get the half-metallic character of the density of states. As discussed previously with the *ab initio* results, a U on the Re d states introduces an effective exchange splitting on the same, resulting in a gain for the ferromagnetic ground state. We probe this fact independently using the model Hamiltonian that we have developed. We calculate the stability of the ferromagnetic ground state with respect to the previously considered antiferromagnetic state with variation of exchange splitting (J_h) at the Re site.

The calculations were done with a fixed U of 0.4 eV of the Re d states and keeping all the other parameters the same as their previous values. The obtained results are tabulated in Table V.

As we can see, with an increase in J_h from 0.24 to 0.35 eV at the Re site, the stability of the ferromagnetic state is indeed

TABLE V. Within a multiband Hubbard model, the obtained change in stability of the ferromagnetic state with respect to closest competing antiferromagnetic state as function of exchange splitting at the Re site for Sr_2FeReO_6.

J_h (eV)	ΔE [AFM-FM] (eV)
0.24	0.134
0.35	0.173
0.50	0.186

enhanced by ∼40 meV. This supports our previously given explanation for increase in the stability of ferromagnetic state with application of U on the Re site as it causes an effective exchange splitting at the Re site. This suggests a route to enhance the T_c of these double perovskite systems by using magnetic atoms at the B' site.

Finally, a comparison with a similar system Sr_2FeMoO_6 (SFMO) has been drawn to explain the role two of electrons present in the Re d orbitals (Re^{5+}) in the case of SFRO. Change in the ferromagnetic stability with respect to the same antiferromagnetic configuration is calculated for SFMO and the results are tabulated in Table II. As one can see that in the case of SFMO, the stability of ferromagnetic state increases when a U of 1 eV is applied at the Mo site, but the gain is much less than that of SFRO. While in the case of SFRO this gain was ∼50 meV, here it is only 14 meV. Further increase of U at the Re site from 1 to 2 eV causes the stability to decrease in the case of SFRO while the stability is nearly constant in the case of SFMO. This weaker effect of U on the Mo site in bringing an effective exchange splitting on it can easily be seen by analyzing the density of states for Fe, Mo d orbitals. The features in the density of states shown in Fig. 11 for the ferromagnetic configuration (left panel) is almost similar to that of the SFRO with the only difference that the weight of Mo d orbitals in SFMO is less at the Fermi level when compared to Re d states in SFRO. This can be understood as the Re atom has two electrons in its d orbitals in the ionic configuration of 5+ while Mo has only one electron in its 4d orbital. In the antiferromagnetic configuration, U of 1 eV on the Mo d has almost no effect on the its density of effects

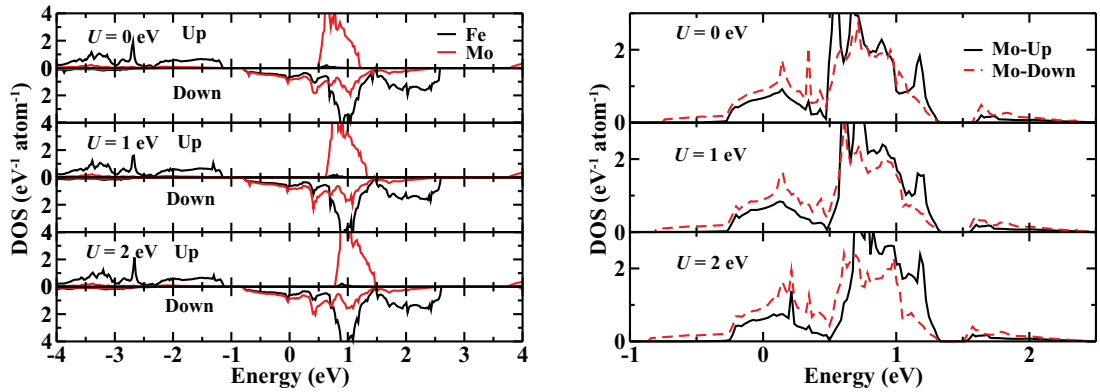


FIG. 11. Atom projected Fe, Mo d density of states plots from *ab initio* calculations for Sr_2FeMoO_6. The plot in the left is obtained for a ferromagnetic configuration of Fe spins while the plot in the right is from the closest competing antiferromagnetic state. The zero of energy is the Fermi energy.

while a U of 2 eV brings only a small change at the Fermi level explaining the less gain in stability of the ferromagnetic state with the variation of U.

IV. CONCLUSIONS

In this study, using *ab initio* electronic structure calculations we have explained the role of electron-electron correlations at the nonmagnetic Re site in Sr_2FeReO_6 in the context of its high ferromagnetic ordering temperature. We show that the role of U on the Re site is to introduce an effective exchange splitting reducing the gain from the antiferromagnetic pathways, providing higher stability to the ferromagnetic ground state. A simple multiband Hubbard like model is developed to independently verify this finding. Within this model, indeed, we find an increase in the stability of the ferromagnetic ground state with increase of exchange splitting at Re site. The role of two electrons of Re d orbitals result in substantial gain of the ferromagnetic stability and this is also contrasted with a similar compound, Sr_2FeMoO_6, which has single d electron at the Mo site.

ACKNOWLEDGMENT

P.M. thanks SERB, Government of India for support through a Project No. IPA/2020/000066.

[1] J. Longo and R. Ward, J. Am. Chem. Soc. **83**, 2816 (1961).
[2] K.-I. Kobayashi, T. Kimura, H. Sawada, K. Terakura, and Y. Tokura, Nature (London) **395**, 677 (1998).
[3] K.-I. Kobayashi, T. Kimura, Y. Tomioka, H. Sawada, K. Terakura, and Y. Tokura, Phys. Rev. B **59**, 11159 (1999).
[4] J. M. D. Coey, M. Viret, and S. Von Molnar, Adv. Phys. **48**, 167 (1999).
[5] D. D. Sarma, P. Mahadevan, T. Saha-Dasgupta, S. Ray, and A. Kumar, Phys. Rev. Lett. **85**, 2549 (2000).
[6] J. Kondo, Prog. Theor. Phys. **32**, 37 (1964).
[7] K. Phillips, A. Chattopadhyay, and A. J. Millis, Phys. Rev. B **67**, 125119 (2003).
[8] J. L. Alonso, L. A. Fernández, F. Guinea, F. Lesmes and V. Martín-Mayor', Phys. Rev. B **67**, 214423 (2003).
[9] G. Jackeli, Phys. Rev. B **68**, 092401 (2003).
[10] L. Brey, M. J. Calderon, S. Das Sarma, and F. Guinea, Phys. Rev. B **74**, 094429 (2006).
[11] O. Erten, O. N. Meetei, A. Mukherjee, M. Randeria, N. Trivedi, and P. Woodward, Phys. Rev. Lett. **107**, 257201 (2011).
[12] P. E. Blöchl, Phys. Rev. B **50**, 17953 (1994).
[13] G. Kresse and D. Joubert, Phys. Rev. B **59**, 1758 (1999).
[14] G. Kresse and J. J. Furthmüller, Phys. Rev. B **54**, 11169 (1996).
[15] J. P. Perdew, K. Burke, and Y. Wang, Phys. Rev. B **54**, 16533 (1996).
[16] S. L. Dudarev, G. A. Botton, S. Y. Savrasov, C. J. Humphreys, and A. P. Sutton, Phys. Rev. B **57**, 1505 (1998).
[17] L. M. Sandratskii, Phys. Status Solidi B **136**, 167 (1986).
[18] S. V. Halilov, H. Eschrig, A. Y. Perlov, and P. M. Oppeneer, Phys. Rev. B **58**, 293 (1998).
[19] O. Grotheer, C. Ederer, and M. Fähnle, Phys. Rev. B **63**, 100401(R) (2001).
[20] M. Ležaić, P. Mavropoulos, G. Bihlmayer, and S. Blügel, Phys. Rev. B **88**, 134403 (2013).
[21] M. Marsman and J. Hafner, Phys. Rev. B **66**, 224409 (2002).
[22] A. K. Nandy, Ph.D. Thesis, University of Calcutta, 2013.
[23] D. Landau and K. Binder, *A Guide to Monte Carlo Simulations in Statistical Physics* (Cambridge University Press, Cambridge, 2000).
[24] N. Metropolis, A. Rosenbluth, M. Rosenbluth, A. Teller, and E. Teller, J. Chem. Phys. **21**, 1087 (1953).
[25] J. C. Slater and G. F. Koster, Phys. Rev. **94**, 1498 (1954).
[26] A. W. Sleight, J. Longo, and R. Ward, Inorg. Chem. **1**, 245 (1962).
[27] H. Kato, T. Okuda, Y. Okimoto, Y. Tomioka, K. Oikawa, T. Kamiyama, and Y. Tokura, Phys. Rev. B **69**, 184412 (2004).
[28] J. C. Slater, Phys. Rev. **34**, 1293 (1929); E. U. Condon, *ibid.* **36**, 1121 (1930); see also, J. S. Griffith, *The Theory of Transition-Metal Ions* (Cambridge University Press, Cambridge, 1961).
[29] S. Nimkar, D. D. Sarma, H. R. Krishnamurthy, and S. Ramasesha, Phys. Rev. B **48**, 7355 (1993).
[30] P. Mahadevan, K. Sheshadri, D. D. Sarma, H. R. Krishnamurthy, and R. Pandit, Phys. Rev. B **55**, 9203 (1997).
[31] S. Middey, A. Kumar Nandy, S. K. Pandey, P. Mahadevan and D. D. Sarma, Phys. Rev. B **86**, 104406 (2012).
[32] A. A. Mostofi, J. R. Yates, Y.-S. Lee, I. Souza, D. Vanderbilt, and N. Marzari, Comput. Phys. Commun. **178**, 685 (2008).
[33] P. Mahadevan, N. Shanthi, and D. D. Sarma, Phys. Rev. B **54**, 11199 (1996).